Biochem. J. (1975) **145**, 93–103
Printed in Great Britain

The Steady-State Kinetics of Peroxidase with 2,2'-Azino-di-(3-ethylbenzthiazoline-6-sulphonic acid) as Chromogen

By ROBERT E. CHILDS and WILLIAM G. BARDSLEY
Department of Obstetrics and Gynaecology, University of Manchester, St. Mary's Hospital, Manchester M13 0JH, U.K.

(*Received* 30 *April* 1974)

The chemical nature of the important new chromogen ABTS [2,2'-azino-di-(3-ethylbenzthiazoline-6-sulphonic acid)] is described together with an account of the redox and spectroscopic properties of the system ABTS–H_2O_2–peroxidase. $K_{eq.}$ is calculated and a study of the steady-state kinetics over a whole range of substrate concentrations is reported. By using novel methods of kinetic analysis, an interpretation of the results is given which requires some extension of the classical peroxidase mechanism.

Peroxidase (EC 1.11.1.7) is a haemoprotein enzyme from horseradish which has been extensively studied by chemical and physical techniques over many years and has proved a useful testing ground for several new theories. The classical phase of this work belongs to the history of the development of enzymology and has been the subject of extensive reviews (Hayaishi, 1962; Paul, 1963; Saunders *et al.*, 1964).

Although doubt remains about the precise description of the chemical events at the active site, there is general agreement that the catalytic sequence involves interaction of enzyme (E) and H_2O_2 (A) to give compound I (EA) followed by addition of reduced chromogen (B) and loss of one-electron-equivalent-oxidized chromogen (P) to give compound II (F). Further addition of B and release of P then regenerates E. Also, excess of A converts compound II into compound III (FA), which is only slowly converted into E by pathways involving B but as yet not fully understood. Oxidizing agents such as alkylhydrogen peroxides can bring about the time-dependent irreversible production of further enzymically inactive complexes such as compound IV, which are artifacts and have no mechanistic significance. Using the nomenclature of Cleland (1963), we have the following Ter Bi Ping Pong mechanism with dead-end substrate inhibition given by A:

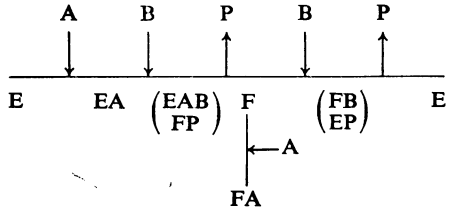

Combination of A with E and F is independent of the nature of B, but the relative rates of the consecutive one-electron transfer processes and conversion of compound III into E will depend on the structure and redox potential of the chromogen B.

Recently, the peroxidase reaction has gained added significance in the field of analytical biochemistry because H_2O_2 produced by oxidase reactions can be used to oxidize a chromogen to give specific and accurate coupled assays for glucose and other substances. Indeed, commercial kits are available for this, but one problem concerns the chromogen. This must be specific for peroxidase, not appreciably inhibit the oxidase enzyme, give a stable product with a well-defined visible absorption spectrum, be chemically stable and, in particular, be non-toxic. All these considerations except the last are met by the usual chromogens. The carcinogenicity of *o*-dianisidine has, however, prompted the search for better chromogens and recently the compound ABTS [2,2'-azino-di-(3-ethylbenzthiazoline-6-sulphonic acid)] has been introduced. We have found this compound to be the chromogen of choice for the assay of peroxidase in cervical mucus and for diamine oxidase activity (J. S. Shindler, R. E. Childs & W. G. Bardsley, unpublished work) and considered a study of the steady-state kinetics of cervical-mucus peroxidase necessary. Finding that the mechanism for this enzyme was more complex than expected, we decided to investigate the steady-state kinetics of the classical horseradish peroxidase with ABTS as chromogen, and the results of this study are presented in the present paper.

Materials and Methods

ABTS was supplied in the form of the crystallized diammonium salt by Boehringer Corporation (London) Ltd., London W.5, U.K., and used without further purification.

Peroxidase was supplied as a salt-free, freeze-dried powder (activity about 60 Sumner purpurogallin

units/mg or 820 units/mg) by BDH Chemicals Ltd., Poole, Dorset.

H_2O_2 solution (100-vol. A.R.) was supplied by Hopkin and Williams, Chadwell Heath, Essex, U.K., and standardized by acid permanganate titration with oxalic acid as primary standard.

The buffer solution used throughout this work was 0.1M-KH_2PO_4 adjusted to pH6.0.

Spectrophotometric measurements

A Cary 118C recording spectrophotometer fitted with automatic cell changer was used and it was found possible to measure rates of change as low as $0.0002E$ unit·min^{-1} by using the $0.02E$ full-scale expansion facility and 5s pen-response mode. Throughout this work, the 0.05, 0.1, 0.2 or $0.5E$ scale expansion was used with electronic zero suppression, chart speed as appropriate, fixed gain, automatic slit-width control and 1s pen-response mode. The linearity and reproducibility of the assay was demonstrated in an experiment with enzyme (50μg·litre^{-1}), ABTS (0.01mM) and H_2O_2 (0.002mM). Ten experiments gave an initial rate of $2.1\times10^{-3}E_{414}$ unit·min^{-1} (S.D. $\pm1.47\times10^{-4}$).

Determination of the molar extinction coefficient of ABTS oxidation product and the equilibrium constant for the reaction

A solution containing peroxidase (0.1μg) in 1ml of buffer, pH6.0, containing 0.05mM-ABTS was incubated in a stoppered cuvette in the thermostatically controlled sample compartment of a Cary 118C spectrophotometer. When the temperature was steady at 37°C, a scan of the cell was obtained between 200nm and 800nm. Then 3μl of H_2O_2 (0.915mM) was added and when the E_{340} of the cell ceased to decrease and the E_{414} to increase, it was presumed that equilibrium had been reached and the cell was again scanned. This procedure was repeated for ten further additions of H_2O_2.

Steady-state measurements

Initial rates were measured over 2min at 20°C in a final volume of 1.0ml of buffer, pH6.0, containing peroxidase (50ng) for 150 combinations of H_2O_2 and ABTS ranging between the limits of H_2O_2 from 0.002 to 56mM and ABTS from 0.01 to 56mM. The lower concentration limit is set by the fact that substrate concentrations lower than this give non-linear initial rates because of substrate depletion, whereas concentrations much greater than 56mM are not possible because of the limited solubility of ABTS.

Graphical methods

The shapes of the graphs of polynomial ratios can often give information about the nature of the polynomial functions. Consider the first and second derivative (Botts, 1958; Ferdinand, 1966; Childs & Bardsley, 1974) for the general 2:2 function

$$y=\frac{\alpha_1 x+\alpha_2 x^2}{\beta_0+\beta_1 x+x^2};\ x\geqslant 0$$

where 2:2 refers to the degree of numerator:denominator in x and α_i, β_i are general positive constant coefficients. This leads to the conclusion that this curve will have $\lim_{x\to\infty}=\alpha_2$ and have (i) no sigmoid inflexions or maxima if

$$\frac{\alpha_1}{\alpha_2}>\frac{\beta_0}{\beta_1}$$

and

$$\frac{\alpha_1}{\alpha_2}<\beta_1$$

(ii) a sigmoid inflexion but no maximum if

$$\frac{\alpha_1}{\alpha_2}<\frac{\beta_0}{\beta_1}$$

and

$$\frac{\alpha_1}{\alpha_2}<\beta_1$$

(iii) no sigmoid inflexion but a maximum if

$$\frac{\alpha_1}{\alpha_2}>\frac{\beta_0}{\beta_1}$$

and

$$\frac{\alpha_1}{\alpha_2}>\beta_1$$

or (iv) sigmoid inflexion and maximum if

$$\frac{\alpha_1}{\alpha_2}<\frac{\beta_0}{\beta_1}$$

and

$$\frac{\alpha_1}{\alpha_2}>\beta_1$$

In addition, when $\alpha_2=0$, the curve can never be sigmoid but must have a maximum and $\lim_{x\to\infty}=0$.

In double-reciprocal form we have the 2:1 function

$$\frac{1}{y}=\frac{\beta_0\left(\frac{1}{x}\right)^2+\beta_1\left(\frac{1}{x}\right)+1}{\alpha_1\left(\frac{1}{x}\right)+\alpha_2}$$

which is a curve approaching a linear asymptote as $\left(\frac{1}{x}\right) \to \infty$ except when $\alpha_1 = 0$, when a parabola results. The curve can be (i) concave upward if

$$\left[1-\beta_1\left(\frac{\alpha_2}{\alpha_1}\right)+\beta_0\left(\frac{\alpha_2}{\alpha_1}\right)^2>0\right]$$

(ii) concave downwards if

$$\left[1-\beta_1\left(\frac{\alpha_2}{\alpha_1}\right)+\beta_0\left(\frac{\alpha_2}{\alpha_1}\right)^2<0\right]$$

and with

$$\frac{\mathrm{d}\left(\frac{1}{y}\right)}{\mathrm{d}\left(\frac{1}{x}\right)} \leqslant 0$$

at the origin in the cases (iii) and (iv) previously. The curve is undefined at the origin for $\alpha_2 = 0$. Now any pair of curves of y against x or $1/y$ against $1/x$ that are not of these shapes can only mean that the original functions are greater than 2:2.

For the general 2:3 function:

$$y = \frac{\alpha_1 x + \alpha_2 x^2}{\beta_0 + \beta_1 x + \beta_2 x^2 + x^3}$$

the double-reciprocal form is:

$$\frac{1}{y} = \frac{1+\beta_2\left(\frac{1}{x}\right)+\beta_1\left(\frac{1}{x}\right)^2+\beta_0\left(\frac{1}{x}\right)^3}{\alpha_2\left(\frac{1}{x}\right)+\alpha_1\left(\frac{1}{x}\right)^2}$$

giving

$$\frac{\mathrm{d}\left(\frac{1}{y}\right)}{\mathrm{d}\left(\frac{1}{x}\right)} = \frac{\beta_0}{\alpha_1} + \frac{(\alpha_1\alpha_2\beta_1 - \alpha_1^2\beta_2 - \alpha_2^2\beta_0)\left(\frac{1}{x}\right)^2 - 2\alpha_1^2\left(\frac{1}{x}\right) - \alpha_1\alpha_2}{\alpha_1\left(\frac{1}{x}\right)^2\left[\alpha_1\left(\frac{1}{x}\right)+\alpha_2\right]^2} \to \frac{\beta_0}{\alpha_1} \quad \text{as} \quad \frac{1}{x} \to \infty.$$

This gradient is greater than β_0/α_1 if

$$\frac{1}{x} > \frac{\alpha_1^2}{a} + \left(\frac{\alpha_1^4}{a^2} + \frac{\alpha_1\alpha_2}{a}\right)^{\frac{1}{2}} > 0; \quad \text{and } a > 0,$$

where $a = \alpha_1\alpha_2\beta_1 - \alpha_1{}^2\beta_2 - \alpha_2{}^2\beta_0$ and so approaches β_0/α_1 from above, i.e. there is an inflexion in the curve $1/y$ against $1/x$ under the condition $a > 0$. Thus an inflected double-reciprocal plot implies a minimum degree of 2:3 in the steady-state equation.

Similarly higher-degree (i.e. 3:3 etc.) functions may have inflexions under appropriate constraints.

In conclusion, we note that where a function has equal degree in numerator and denominator [$y/(x)$ reaches horizontal non-zero asymptote], then curves of y against x with horizontal plateaux or multiple maxima or curves of $1/y$ against $1/x$ with inflexions imply functions with minimum degree of 3:3. Since enzyme mechanisms with two substrates (say, A, B as in the present case) always give rate equations of the form

$$v = \frac{ABf(A,B)}{g(A,B)}$$

in the absence of products where A and B represent concentration of species A and B, we can use the above reasoning to discover the minimum degree of A and B. Also, it is found that when double-reciprocal plots reach linear asymptotes, the slopes of these asymptotes are polynomial ratios in the fixed substrate. Thus the slopes of $1/v$ against $1/A$ will be of the form

$$\text{slope} = \frac{1+\beta_1 B+\beta_2 B^2+\cdots\beta_m B_m}{\alpha_1 B+\alpha_2 B^2+\cdots\alpha_n B^n}$$

and we can apply the same type of reasoning to these graphs. A similar argument could be made for the functions describing the horizontal asymptotes from plots of v against A as functions of B and of v against B as functions of A. (Note that axis-intercept replots are of higher degree and are of less assistance in determining mechanism.)

Stoichiometry of the reaction coupled with the above analysis provides a powerful tool in mechanistic interpretation.

Results

The redox chemistry of ABTS is illustrated in Fig. 1. Two molecules of ABTS (I) react with one of H_2O_2 giving two molecules of radical cation (II). The radical cation slowly disproportionates to give one molecule each of species (I) and azodication (III) which can also undergo further reactions in alkaline solution. We have attempted to prepare the product by chromatography in order to pursue product-inhibition studies but have failed to obtain a pure sample. However, as will become clear below, the catalytic mechanism is random, and product-inhibition patterns would be ambiguous.

Fig. 2(*a*) shows the repeat scans over the wavelength range 300–460nm when the reaction has reached equilibrium after addition of H_2O_2. Results indicate that ABTS has an absorption maximum at

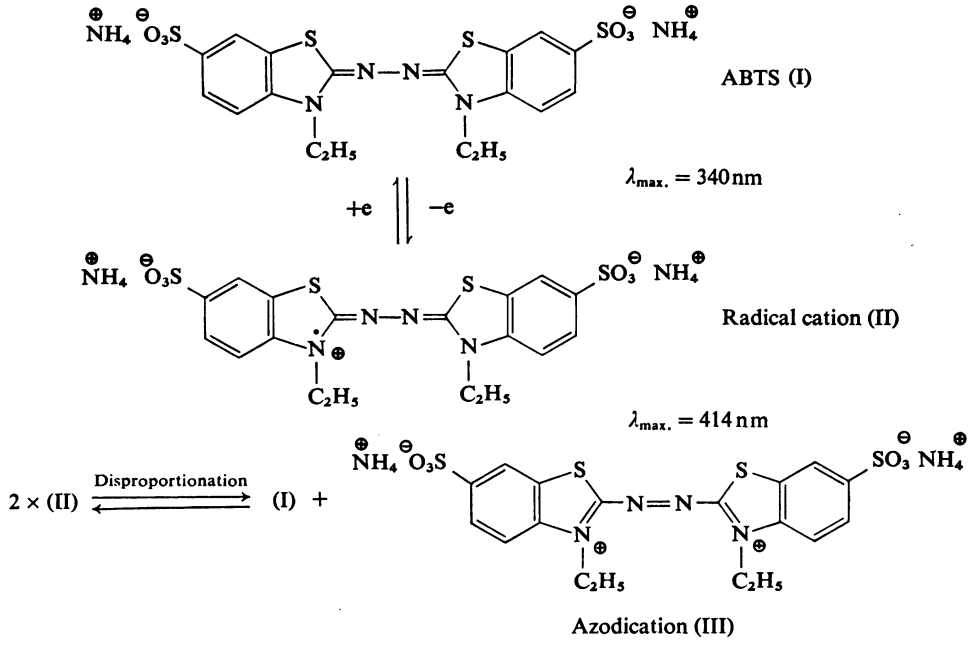

Fig. 1. *Chemical formulae of ABTS and its oxidation products*

ABTS (I) can undergo a one-electron oxidation to give the metastable radical cation (II), which slowly disproportionates giving (I) and the azodication (III). This last chemical change is too slow to affect initial-rate measurements but becomes a complicating factor when equilibrium studies lasting several hours are conducted or when attempts are made to purify compound (II) for product inhibition studies.

340nm ($\varepsilon = 3.6\times10^4 M^{-1}\cdot cm^{-1}$) and the radical cation has an absorption maximum at 414nm ($\varepsilon = 3.6\times10^4 M^{-1}\cdot cm^{-1}$) together with lesser maxima at 395, 640 and 725nm and a shoulder at 580nm. When the decrease in E_{340} is plotted against the increase in E_{414} and the values are corrected for the fact that the radical cation has an E_{340} of 15% of E_{414}, and are also corrected for time-dependent decay of the 414nm peak due to disproportionation, a straight line is obtained. From 33 experimental points, a mean value of $K_{eq.} = [P]^2/[A][B]^2 = 3.0\times10^5$ litre$\cdot M^{-1}$ (S.D. $\pm 1.0\times10^5$) was calculated where A is H_2O_2, B is ABTS and P the radical cation. These corrections are not normally necessary in kinetic studies where rates were obtained over 2min, but were required in this experiment owing to the long time-intervals required to ensure equilibrium conditions between each successive scan. The rate of decay of the 414nm peak at the conclusion of the experiment was $0.007E$ unit$\cdot$ min^{-1}. The efficiency of ABTS as hydrogen donor in the peroxidase reaction is seen by comparing the rates of change at appropriate wavelengths by using H_2O_2 (2mM) and chromogen (2mM), which were ABTS (100%), *o*-dianisidine (5.32%), pyrogallol (1.08%), 4-aminophenazine (0.0016%) and guaiacol (0.006%).

Fig. 2(*b*) shows the spectral change obtained when ABTS is added to peroxidase in the absence of H_2O_2, indicating the formation of a peroxidase–ABTS complex.

Figs. 3 and 4 show a selection of the experimental data obtained. Because of the enormous concentration range used in this study, it is not possible to show all experimental points on any one graph, but sufficient points are plotted to display the shape of each individual graph, and further discussion now concerns the implications derived from these shapes when interpreted in the light of the previous discussion of the graphs of polynomial functions. Similar sets of curves have been obtained on many separate occasions, sometimes in duplicate, sometimes in triplicate. The unusual shapes are definitely not artifacts.

Discussion

(1) *The peroxidase reaction*

The catalytic sequence will now be discussed with reference to Fig. 5 which contains the classic peroxidase mechanism (heavy lines), the pathway via compound III (ordinary lines), a random pathway (barred line), which we propose to account for the

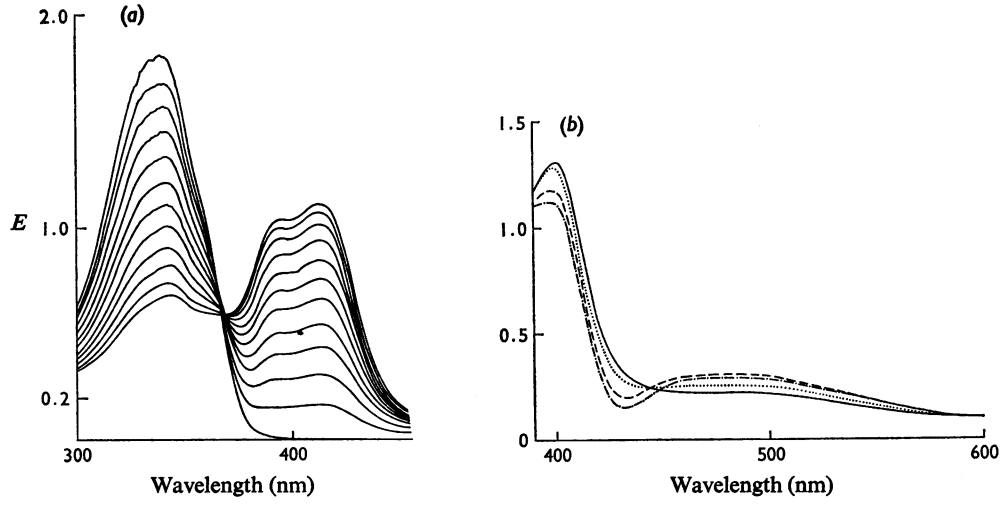

Fig. 2. *Determination of $K_{eq.}$ and ε for the radical cation by spectrophotometric titration*

(*a*) A solution of 0.05 mM-ABTS containing peroxidase (0.1 μg) in 1 ml of KH_2PO_4 buffer, pH 6.0, at 37°C was titrated by stepwise addition of 3 μl batches of H_2O_2 (0.915 mM). When equilibrium had been reached, a wavelength scan of the cuvette was obtained. Information from Fig. 2(*a*) was corrected for time-dependent decay of the 414 nm peak and contribution of the radical cation to E_{340}. The experiment was performed in triplicate and the linear relationship between the absorbance changes gives $\varepsilon_{ABTS} = \varepsilon_{Radical\ cation} = 3.6 \times 10^4$ for a 1 cm path-length. Movement of the isosbestic point towards the end of the experiment is due to time-dependent decay of the radical cation. (*b*) Absorption spectrum of peroxidase (2 mg·ml^{-1}) at pH 6.0 in aerobic solutions of: ——, buffer; ····, ABTS (2 mM); ----, ABTS (8 mM); –·–·, ABTS (20 mM). Addition of further ABTS produced no additional change in the spectrum.

degree of A and B in the rate equations, an 'escape pathway' (dashed line) which we propose in order to explain the fact that substrate inhibition given by A is partial (plots of v against [A] reaching horizontal non-zero asymptotes) and not dead-end, and an extra pathway (dotted line) which is suggested by the failure to detect compound I as being on the main pathway from compound III to E on addition of B.

The pathway (1)—(2)—(4)—(5)—(6) is unquestionably the main catalytic sequence. Node (1) is the free enzyme (ferric peroxidase) which has been extensively investigated for isoenzymes (Shannon *et al.*, 1966) and (2) is compound I, which is thought to be a derivative in which the active site is oxidized rather than a simple enzyme–substrate complex (Schonbaum & Lo, 1972). In addition to this well-characterized sequence, the conversion of (5) (compound II) into (7) (compound III) by excess of H_2O_2 (George, 1953) merits special comment. This compound is thought to be oxyperoxidase which can be prepared from ferrous peroxidase and O_2 (Wittenburg *et al.*, 1966), from dihydroxyfumarate and ferric peroxidase (Theorell & Swedin, 1940; Chance, 1952) or from ferrous peroxidase in the presence of NADH, especially at acidic pH (Yamazaki & Yokota, 1965). Compound III undergoes slow spontaneous first-order decay to give ferric peroxidase without detectable intermediates, and the decay is accelerated by both electron donors and electron acceptors (Yokota & Yamazaki, 1965). In concentrated enzyme solutions, there are many complex interactions between different enzyme species leading to the disappearance of compound III (Tamura & Yamazaki, 1972; Yamazaki & Yokota, 1973), but it is unlikely that these reactions are of any significance at the extremely low enzyme concentrations used in our steady-state work. Although the reaction

$$\text{Compound III} + e + 2H^+ \rightarrow \text{peroxidase} + H_2O_2$$

has been suggested (Yokota & Yamazaki, 1965), there is confusion about the intermediates involved which have proved difficult to identify. We suggest that the sequence (7)—(8) followed by (8)—(6) or (8)—(2) is reasonable.

It seems that addition of electron donor to enzyme could occur before addition of H_2O_2 if the donor had sufficient affinity, and this would be the sequence (1)—(3)—(4), for which there has been no evidence previously. Now most of the electron donors used so far are much less efficient than ABTS and even 3,3′-diaminobenzidine, which has recently been claimed as the best donor (Herzog & Fahimi, 1973) is much less efficient than ABTS. Consequently, the failure to recognize the sequence (1)—(3)—(4)

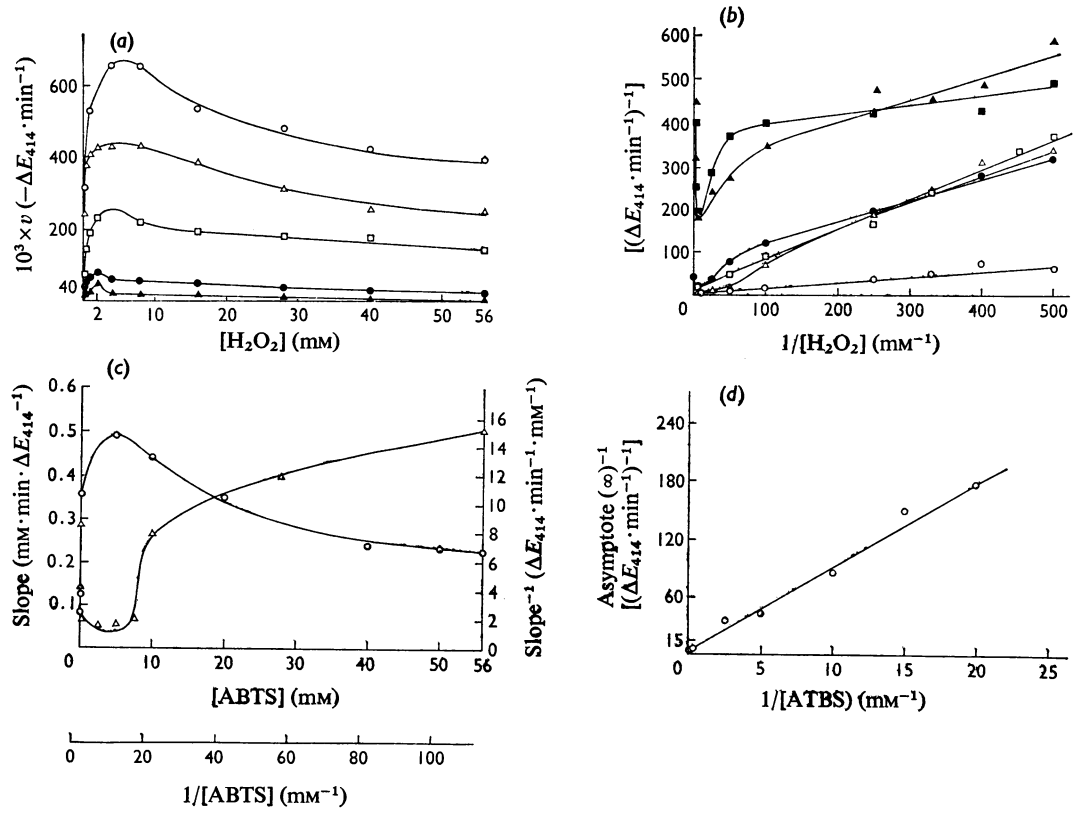

Fig. 3. *Primary and derived plots for H_2O_2*

(*a*) Plots of v against $[H_2O_2]$ for various concentrations of second substrate (ABTS). Concentrations of ABTS shown are: ○, 28mM; △, 10mM; □, 5mM; ●, 0.2mM; ▲, 0.05mM. (*b*) Double-reciprocal plots of $1/v$ against $1/[H_2O_2]$ for various concentrations of ABTS. Concentrations of ABTS are: ○, 10mM; △, 7.5mM; □, 2.5mM; ●, 0.2mM; ▲, 0.05mM; ■, 0.01mM. (*c*) Slope replots from (*b*). These slopes were taken from the asymptotes on (*b*) and related graphs at high values of $1/[H_2O_2]$. ○, Slope against 1/[ABTS]; △, 1/slope against [ABTS]. (*d*) Replot of reciprocal of asymptotic values of v for large $[H_2O_2]$, taken from (*a*) and related graphs, against 1/[ABTS] showing a straight line and hence implying 1:1 in ABTS.

previously does not constitute a problem. Titration of peroxidase with ABTS in the absence of H_2O_2 produces a slight decrease in E_{400} and a progressive increase in E_{480} which reaches a maximum at ABTS concentrations above 8mM (Fig. 2*b*), which may be due to the formation of (3).

Other recent studies with peroxidase have included detailed study of the chemistry of artificial peroxidases (Ohlsson & Paul, 1973; Makino & Yamazaki, 1972, 1973) and a study of the reaction mechanism and interaction between peroxidase species by pulse radiolysis (Bielski *et al.*, 1974) and stopped-flow techniques (Phelps *et al.*, 1974), but we are not aware of any recent definitive steady-state kinetic studies. Preliminary steady-state kinetics have been reported, however, for horseradish peroxidase with phenol as hydrogen donor (Danner *et al.*, 1973) and crayfish peroxidase with guaiacol and *o*-dianisidine (Hartenstein, 1973).

(2) *Interpretation of the kinetic experiments*

From Fig. 3(*a*) we conclude that the degree of A in the rate equation is equal in both numerator and denominator (as the curves become horizontal for large [A]) and that the degree is at least 2:2 in A, since each of the curves has a maximum.

From Fig. 3(*b*) (the double-reciprocal plot of Fig. 3*a*), we see that the degree of A in the rate equation must be greater than 2:2, i.e. at least 3:3, since the curves have inflexions, and further, since they approach straight lines asymptotically, there is a linear term in A in the numerator.

From Fig. 3(*c*) (slope replots of Fig. 3*b*), again

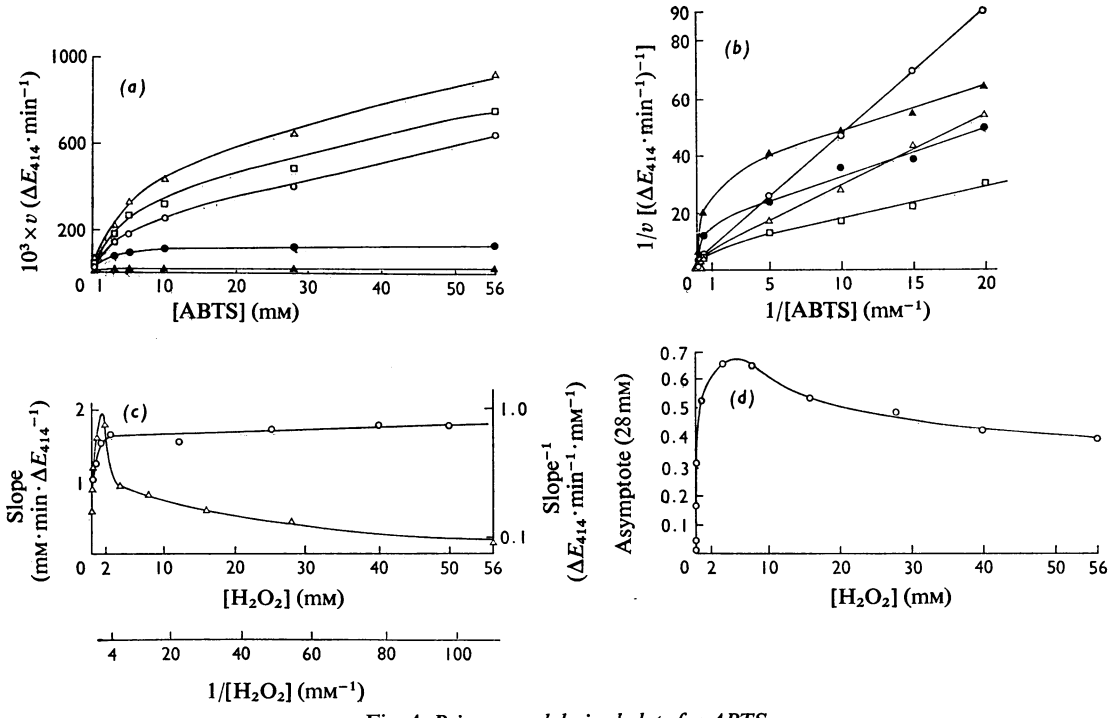

Fig. 4. *Primary and derived plots for ABTS*

(*a*) Plots of v against [ABTS] for various concentrations of second substrate (H_2O_2). Concentrations of H_2O_2 shown are: ○, 56mM; □, 28mM; △, 8mM; ●, 0.2mM; ▲, 0.002mM. (*b*) Double-reciprocal plots of $1/v$ against 1/[ABTS] for various concentrations of H_2O_2. Concentrations of H_2O_2 are: ○, 28mM; △, 8mM; □, 2mM; ●, 0.2mM; ▲, 0.04mM. (*c*) Slope replots from (*b*). The slopes were taken from the asymptotes on (*b*) and similar graphs at high values of 1/[ABTS]. ○, Slope against 1/[H_2O_2]; △, 1/slope against H_2O_2. (*d*) ○, Asymptotic value of v for large [ABTS] plotted against [H_2O_2] taken from (*a*) and related graphs.

because of the inflexions in the double-reciprocal form (triangles), we conclude that B in the rate equation is of degree at least 3:3.

From Fig. 3(*d*) (horizontal asymptotes of Fig. 3*a*) we see that $\lim_{A\to\infty} v(A,B)$ is 1:1 in B.

Similar analysis of Figs. 4(*a*), 4(*b*), 4(*c*) and 4(*d*) lead to the following conclusions. The degree of B in the rate equation is equal in both numerator and denominator (Fig. 4*a*), there is a linear term in B in the numerator (Fig. 4*b*, straight-line asymptotes), and the degree of B is at least 2:2 (Fig. 3*c*, however, increases this to 3:3). The degree of A is now seen to be greater than that of B in the original rate equation (compare Figs. 3*d* and 4*d*) and this must be at least 4:4 (Figs. 4*c* and 4*d*).

(3) *A plausible reaction scheme*

We now seek a reaction sequence that is chemically reasonable, accords well with the classical mechanism, has no dead-end complexes, has partial substrate inhibition given by excess of A but not excess of B and is described by a rate equation at least 4:4 in A and 3:3 in B with linear A and B terms in numerator and denominator and which also gives an asymptote for A which is a 1:1 function in B and an asymptote for B which is at least 2:2 in A.

Consider the greater cyclic mechanism of Fig. 5, which has eight nodes corresponding to eight enzyme species and contains several lesser cycles. The cycle (1)→(2)→(4)→(5)→(6)→(1) is the classical peroxidase mechanism. Now, if an enzyme can bind two substrates A and B, it is reasonable to suppose that either of the substrates can bind to the enzyme before the ternary complex is formed. In other words, random addition of A or B to produce EAB is thermodynamically necessary in the absence of enzyme isomerization and accords better with the principle of microscopic reversibility than does strictly ordered addition. Many enzymes have been thought to be ordered until more rigorous examination reveals the random nature and shows that

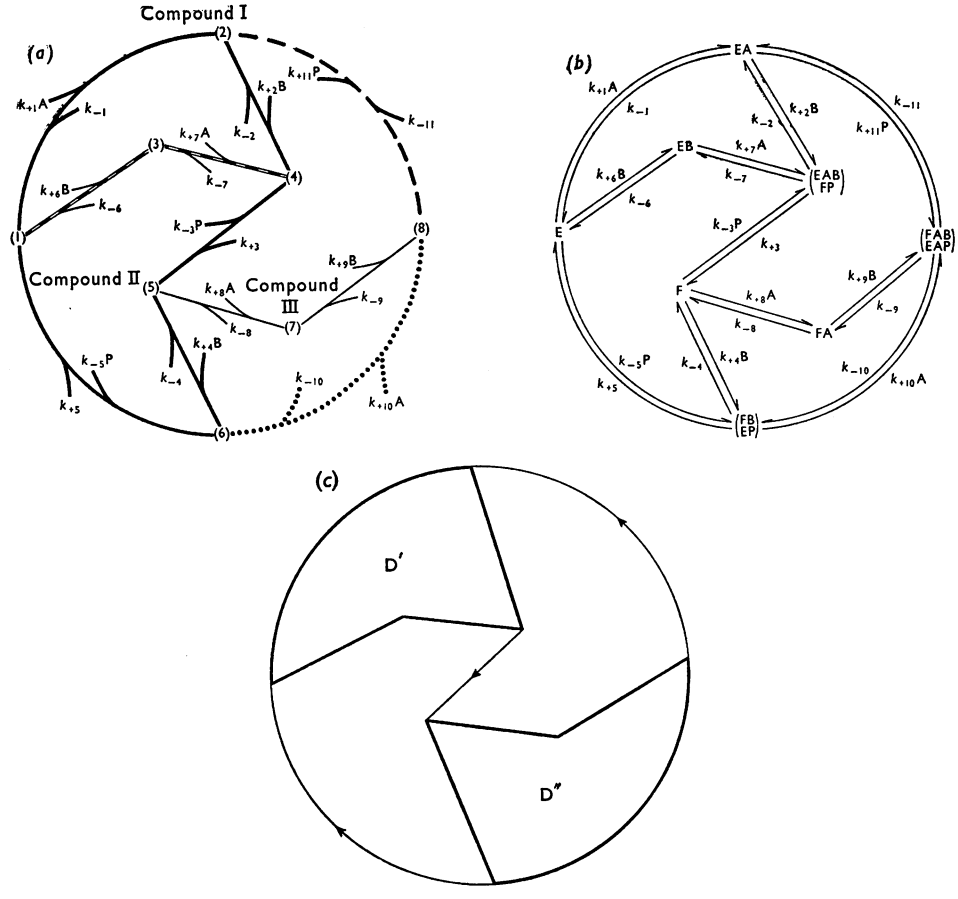

Fig. 5. *Proposed mechanism for horseradish peroxidase with H_2O_2 (A) and ABTS (B)*

(*a*) Diagrammatic representation of the greater cyclic and lesser cyclic mechanisms. The nodes are as follows: (1) E; (2) EA (compound I); (3) EB; (4) $\binom{\text{EAB}}{\text{FP}}$; (5) F (compound II); (6) $\binom{\text{FB}}{\text{EP}}$; (7) FA (compound III); and (8) $\binom{\text{FAB}}{\text{EAP}}$. The greater cycle contains the classical peroxidase sequence (1-2-4-5-6 thick line, ——), and addition of the segmental line (=—=) (1-3-4) gives a random sequence which is favoured under conditions of saturation by B. Saturation with A diverts the reaction flux into the sequence given by narrow black lines (5-7-8, ——) and the dashed sequence (8-2, – – – –) is necessary to avoid dead-end substrate inhibition by A. The dotted line (6-8, · · · ·) is required for stoichiometric reasons and its omission would decrease by one the degree of A in numerator and denominator of the rate equation. (*b*) Conventional representation of the peroxidase mechanism for comparison with the diagrammatic representation. (*c*) The diagram with D′ and D″ is discussed in the text and is useful in calculating a rate equation for the proposed reaction sequence.

kinetic experiments only indicate ordered addition because one pathway is kinetically more favoured than another (Fisher *et al.*, 1972). If, in the present case, we have the sequence (1)→(3)→(4) we are not aware of any classical experiment which would have uncovered this, since spectroscopic and other investigations were conducted with substrates which may have had a much slower (1)→(3)→(4) pathway than with ABTS. We suggest that a random section

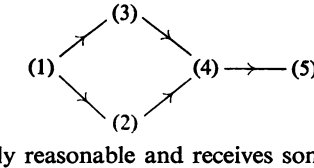

is chemically reasonable and receives some support from experiments that we have now described and from the fact that there is an increasing tendency to find random pathways. This has been shown to be

the case with peroxidase from cervical mucus (J. S. Shindler, R. E. Childs & W. G. Bardsley, unpublished work). The section (5)→(7) followed by some conversion back into (1) is already part of the classical scheme, although no precise description of the intermediates involved in this process have been given and the segments

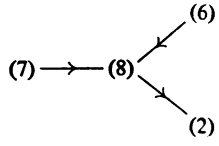

are stoichiometrically realistic.

Suppose that the main sequence was the classical scheme. If the loop (1)→(3)→(4) exists, it would be increasingly favoured by high concentrations of B, and since no substrate inhibition is given by excess of B, this pathway must, in the special case where B is ABTS, be comparable with the classical sequence. We know that excess of A drives the section (5)→(7), but that this cannot be dead-end. The section

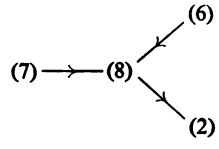

will operate as indicated in the presence of excess of A and, since we know this pathway to be a slower one, the partial substrate inhibition is explained. If the section (8)→(2) is omitted, then dead-end substrate inhibition results from driving the reaction flux into the unproductive node (8), which is inconsistent with the kinetic results. Likewise, the section (7)→(8) is necessary to avoid dead-end substrate inhibition by A, and when this is allowed, the section (8)→(6) becomes mandatory from considerations of stoichiometry and kinetics.

(4) *Derivation of the rate equations*

The formidable problem of calculating a rate equation for Fig. 5 is somewhat eased if P is set equal to zero because symmetry between the nodes can be exploited by the procedures of Vol'kenshtein & Gol'shtein (1966) and King & Altman (1956). The resulting rate equation is extremely valuable, since by choosing appropriate values for selected rate constants, we can generate the rate equation for any of the required lesser cycles from such an equation.

In the greater cyclic mechanism proposed for horseradish peroxidase (Fig. 5), let the two lesser cyclic subunits with nodes (1) (2) (4) (3) and (5) (6) (8) (7) be denoted by D′ and D″ respectively. Then we may evaluate the distribution expressions at each node of these subunits as:

$$D'_1 = k_{-1}k_{-2}k_{+7}[A]+k_{-1}k_{-2}k_{-6}+k_{-1}k_{-7}k_{-6}+k_{+2}k_{-7}k_{-6}[B]$$

$$D'_2 = k_{-2}k_{+6}k_{+7}[A][B]+k_{-2}k_{+1}k_{+7}[A]^2+k_{-2}k_{+1}k_{-6}[A]+k_{-6}k_{-7}k_{+1}[A]$$

$$D'_3 = k_{+1}k_{+2}k_{-7}[A][B]+k_{+6}k_{+2}k_{-7}[B]^2+k_{+6}k_{-1}k_{-7}[B]+k_{-1}k_{-2}k_{+6}[B]$$

$$D'_4 = k_{+1}k_{-6}k_{+2}[A][B]+k_{+1}k_{+7}k_{+2}[A]^2[B]+k_{+6}k_{+2}k_{+7}[A][B]^2+k_{-1}k_{+6}k_{+7}[A][B]$$

$$D''_5 = k_{-8}k_{-9}k_{+10}[A]+k_{-8}k_{-9}k_{-4}+k_{-8}k_{-10}k_{-4}+k_{+9}k_{-10}k_{-4}[B]$$

$$D''_6 = k_{+8}k_{+9}k_{-10}[A][B]+k_{+4}k_{+9}k_{-10}[B]^2+k_{-8}k_{-10}k_{+4}[B]+k_{-8}k_{-9}k_{+4}[B]$$

$$D''_7 = k_{+4}k_{+10}k_{-9}[A][B]+k_{+10}k_{-9}k_{+8}[A]^2+k_{-4}k_{-9}k_{+8}[A]+k_{-4}k_{-10}k_{+8}[A]$$

$$D''_8 = k_{-8}k_{+4}k_{+10}[A][B]+k_{+9}k_{+4}k_{+10}[A][B]^2+k_{+9}k_{+8}k_{+10}[A]^2[B]+k_{-4}k_{+8}k_{+9}[A][B]$$

To find the initial rate equation, we put [P] = 0 and evaluate each of the distribution functions D_i for the ith node.

Using the graph process of Vol'kenshtein & Gol'shtein (1966) with node (1) or (2) as an auxiliary, we readily see that

$$D_6 = D'_4 k_{+3} D''_6$$
$$D_7 = D'_4 k_{+3} D''_7$$
$$D_8 = D'_4 k_{+3} D''_8$$

where D_t is the full distribution expression for the relevant node of the complete mechanism.

Similarly, it is found by means of node (6) that

$$D_3 = D''_8 k_{-11} D'_3 + k_{+5} D'_3 R_1$$
$$D_4 = D''_8 k_{-11} D'_4 + k_{+5} D'_4 R_1$$

where

$$R_1 = D''_6 + k_{-11}(k_{+4}[B]k_{+9}[B]+k_{+4}[B]k_{-8}+k_{+9}[B]k_{+8}[A])$$

Also,

$$D_5(\text{auxiliary 1}) = D'_4 k_{+3} R_2$$

$$D_2(\text{auxiliary 6}) = k_{+5} D'_2 R_3 + k_{-11} D''_8 R_4 + k_{+5}k_{+6}k_{+7}k_{+3}k_{+8}k_{+9}k_{-11}[A]^2[B]^2$$

$$D_1(\text{auxiliary 8}) = k_{-11} D'_1 R_5 + k_{+5} D''_6 R_6 + k_{-11}k_{+2}k_{+3}k_{+4}k_{+5} R_7 [B]^2$$

where

$$R_2 = D''_5 + k_{+5}[k_{-8}(k_{-10}+k_{-11})+k_{+9}[B](k_{-10}+k_{-11})+k_{-8}k_{-9}]+k_{-11}k_{+10}[A](k_{-8}+k_{+9})$$

$$R_3 = D''_6 + k_{-11}(k_{-8}k_{+4}[B]+k_{+8}k_{+9}[A][B]+k_{+4}k_{+9}[B]^2)$$

$$R_4 = D'_2 + k_{+3}(k_{+1}k_{-6}[A]+k_{+7}k_{+6}[A][B]+k_{+1}k_{+7}[A]^2)$$

$$R_5 = D''_8 + k_{+5}(k_{-8}k_{+4}[B]+k_{+8}k_{+9}[A][B]+k_{+4}k_{+9}[B]^2)$$

$$R_6 = D'_1 + k_{+3}(k_{-1}+k_{+2}[B])(k_{-6}+k_{+7}[A])$$

$$R_7 = (k_{-8}+k_{+9}[B])(k_{-6}+k_{+7}[A])$$

The initial rate equation is then

$$v = \frac{(k_{+3}D_4 + k_{+5}D_6 + k_{-11}D_8)E_0}{\sum_1^8 D_i}$$

which has the form (on cancelling B):

$$v = \frac{AB(\alpha_0 + \alpha_1 B + \alpha_2 B^2 + \alpha_3 A + \alpha_4 AB + \alpha_5 AB^2 + \alpha_6 A^2 + \alpha_7 A^2 B + \alpha_8 A^3)}{(\beta_0 + \beta_1 B + \beta_2 B^2 + \beta_3 B^3 + \beta_4 A + \beta_5 AB + \beta_6 AB^2 + \beta_7 AB^3 + \beta_8 A^2 + \beta_9 A^2 B + \beta_{10} A^2 B^2 + \beta_{11} A^2 B^3 + \beta_{12} A^3 + \beta_{13} A^3 B + \beta_{14} A^3 B^2 + \beta_{15} A^4 + \beta_{16} A^4 B)} \quad (1)$$

We can see immediately that eqn. (1), which is 4:4 in A and 3:3 in B, satisfies Figs. 3(*a*), 3(*b*), 4(*a*) and 4(*b*), and we examine it further to see if Figs. 3(*c*), 3(*d*), 4(*c*) and 4(*d*) are satisfied.

We find that a plot of $1/v$ against $1/[B]$ approaches a straight line of slope

$$\frac{\beta_0 + \beta_4 A + \beta_8 A^2 + \beta_{12} A^3 + \beta_{15} A^4}{\alpha_0 A + \alpha_3 A^2 + \alpha_6 A^3 + \alpha_8 A^4}$$

i.e. 1/slope against A is 4:4 passing through the origin and slope against $1/[A]$ approaches a straight line for large $1/[A]$ (cf. Fig. 4*c*).

Similarly a plot of $1/v$ against $1/A$ approaches a straight line of slope

$$\frac{\beta_0 + \beta_1 B + \beta_2 B^2 + \beta_3 B^3}{\alpha_0 B + \alpha_1 B^2 + \alpha_2 B^3}$$

so that 1/slope against B is 3:3 passing through the origin and slope against $1/B$ approaches a straight line for large $1/B$ (cf. Fig. 3*c*).

Note also that for large A, v approaches $\alpha_8 B/(\beta_{15} + \beta_{16} B)$ which compares with Fig. 3(*d*), and that for large B, v approaches $(\alpha_2 A + \alpha_5 A^2)/(\beta_3 + \beta_7 A + \beta_{11} A^2)$, which compares with Fig. 4(*d*).

The classical peroxidase equation with random addition of A or B may be derived from eqn. (1) by setting $k_{+8} = k_{+9} = k_{+10} = k_{-11} = 0$ and cancelling the factor $k_{-8}(k_{-9} + k_{+10})$ and is 2:2 in A and B. Further, setting $k_{+6} = k_{+7} = k_{-7} = 0$ and cancelling k_{-6} gives the classical peroxidase mechanism which is 1:1 in A and B, and it is obvious that these equations are of insufficiently high degree in both A and B to account for the experimentally observed behaviour.

Conclusion

We conclude that with ABTS as chromogen, the hitherto unsuspected complexity of the peroxidase reaction sequence has been uncovered.

The greater cyclic mechanism in Fig. 5 contains the classic sequence (1)—(2)—(4)—(5)—(6)—(1), but higher concentrations of ABTS drive the sequence into the alternative cycle (1)—(3)—(4)—(5)—(6)—(1), which is of comparable catalytic efficiency in the special case of ABTS. Excess of H_2O_2 produces partial substrate inhibition by diverting the reaction sequence into the slower catalytic loop

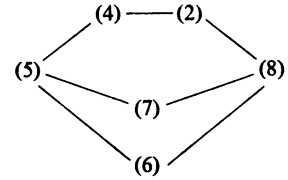

The rate equation given by this scheme is of degree 4:4 in A and 3:3 in B and fully accounts for the steady-state kinetic results. It is impossible to omit any of the sections of the scheme in Fig. 5 without producing features which cannot be reconciled with the experimental findings. For instance, removal of the random section or (7)—(8)—(6) decreases the degree of A and B by one, and removal of the pathway (8)—(2) leads to dead-end substrate inhibition by A, contradicting the observed partial substrate inhibition. Deletion of the pathway (8)—(6) also decreases the degree of A by one in both numerator and denominator.

We thank Professor V. R. Tindall for supporting this project, the Medical Research Council for a grant towards the purchase of a Cary 118C spectrophotometer used in this work, Mr. J. S. Shindler for expert advice, Mr. T. J. Lowe of Boehringer Corp. (London) Ltd. for providing us with technical information about the chromogen used in this project, and Mrs. J. Crombie for expert typing of the manuscript.

References

Bielski, B. H. J., Comstock, D. A., Haber, A. & Chan, P. C. (1974) *Biochim. Biophys. Acta* **350**, 113–120
Botts, J. (1958) *Trans. Faraday Soc.* 593–604
Chance, B. (1952) *Arch. Biochem. Biophys.* **41**, 404–414
Childs, R. E. & Bardsley, W. G. (1974) *J. Theor. Biol.* in the press
Cleland, W. W. (1963) *Biochim. Biophys. Acta* **67**, 104–137
Danner, D. J., Brignac, P. J. & Arceneaux, D. (1973) *Arch. Biochem. Biophys.* **156**, 759–763
Fisher, J. R., Priest, D. G. & Barton, J. S. (1972) *J. Theor. Biol.* 335–352
Ferdinand, W. (1966) *Biochem. J.* **98**, 278–283
George, P. (1953) *J. Biol. Chem.* **201**, 427–434

Hartenstein, R. (1973) *Comp. Biochem. Physiol.* **45B**, 749–762
Hayaishi, O. (1962) *Oxygenases*, Academic Press, New York and London
Herzog, V. & Fahimi, H. D. (1973) *Anal. Biochem.* **55**, 554–562
King, E. L. & Altman, C. (1956) *J. Phys. Chem.* **60**, 1375–1379
Makino, R. & Yamazaki, I. (1972) *J. Biochem. (Tokyo)* **72**, 655–664
Makino, R. & Yamazaki, I. (1973) *Arch. Biochem. Biophys.* **157**, 356–368
Ohlsson, P. I. & Paul, K. G. (1973) *Biochim. Biophys. Acta* **315**, 293–305
Paul, K. G. (1963) *Enzymes* **8**, 227–274
Phelps, C. E., Antonini, E., Giacometti, G. & Brunori, M. (1974) *Biochem. J.* **141**, 265–272
Saunders, B. C., Holmes-Siedle, A. G. & Stark, B. P. (1964) *Peroxidase*, Butterworths, London
Schonbaum, G. R. & Lo, S. (1972) *J. Biol. Chem.* **247**, 3353–3360
Shannon, L. M., Kay, E. & Lew, J. Y. (1966) *J. Biol. Chem.* **241**, 2166–2172
Tamura, M. & Yamazaki, I. (1972) *J. Biochem.* **71**, 311–319
Theorell, J. & Swedin, B. (1940) *Nature (London)* **143**, 71
Vol'kenshtein, M. V. & Gol'shtein, B. N. (1966) *Biochim. Biophys. Acta* **115**, 471–477
Wittenburg, J. B., Noble, R. W., Wittenburg, B. A., Antonini, E., Brunori, M. & Wyman, J. (1966) *J. Biol. Chem.* **242**, 626–634
Yamazaki, I. & Yokota, K. (1965) *Biochem. Biophys. Res. Commun.* **19**, 249–254
Yamazaki, I. & Yokota, K. (1973) *Mol. Cell. Biochem.* **2**, 39–52
Yokota, K. & Yamazaki, I. (1965) *Biochem. Biophys. Res. Commun.* **18**, 48–53